

SuperEMFL

Superconducting magnets for the European Magnet Field Laboratory

Grant Agreement n° 951714
Research and Innovation Action

**Deliverable D3.1 Electrical, thermal and mechanical HTS
conductor properties
[intermediate version]**

Start date of the project: 1st January 2021

Duration: 48 months

Project Coordinator: Xavier Chaud – CNRS LNCMI (P1 - CNRS)

Contact: xavier.chaud@lncmi.cnrs.fr



Document Classification

Title	Electrical, thermal and mechanical HTS conductor properties
Deliverable	D3.1
Reporting Period:	PR1
Date of Delivery foreseen in DoA	Project Month 24, 31 12 2022
Actual Date of Delivery to EC	Project month 8, 05 05 2023
Authors	M. Dhalle, P07 – UT
Work package	WP3 Materials Testing
Dissemination	PU
Type	R
Version	Intermediate version v2
Doc ID Code	D3.1_SuperEMFL_P07_UT_230505
Keywords	Report

Document History

Partner	Remark	Version	Date
P07 UT	Draft	v1	29 03 2023
P01 CNRS	final version	V2	05 05 2023

Document Validation

Partner	Approval (Signature or e-mail reference)
P01 CNRS	Xavier Chaud
P02 HZDR	Thomas HERRMANNSSDOERFER
P03 RU	Uli ZEITLER
P04 CEA	Philippe FAZILLEAU
P05 EMFL	Uli ZEITLER
P06 UNIGE	Carmine SENATORE
P07 UT	Marc DHALLE
P08 IEE	Enric PARDO
P09 TH	Anis SMARA
P10 OI	John BURGOYNE
P11 NOELL	Philipp REVILAK

Document Abstract

This D3.1 deliverable represents an intermediate version that the SuperEMFL consortium decided to publish being aware that the work on both tasks 3.1 and 3.3 have not been concluded yet. The report presents the analysis on Theva tape but in 2023 other tapes will be tested and included in the final version of this D3.1.

Within task 3.3 (*Conductor procurement*), partner 09 TH adapted their HTS tape manufacturing process to meet the requirements of high-field magnets (introducing artificial pinning and physical-vapour deposition of the protection layer for increased performance; and laser-based cutting for enhanced geometry control).

Within task 3.1 (*HTS conductor characterization*), samples of this new tape material were distributed for characterization at the specialized partner labs. The samples were tested - specifically in terms of current-carrying capacity at low temperatures and high magnetic field - by partners 06,07 and 08 (UNIGE, UT and IEE) with assistance of partners 01 and 03 (CNRS and RU), who put to the tasks' disposal their very-high magnetic field facilities. The enhanced properties of the new TH tapes were confirmed and the production of the longer lengths required for task 3.4 (*Small scale model coil manufacture*) was started.

Abbreviations

APC: Artificial Pinning Centers

B : Magnetic flux density

EM: Electro-Magnetic

H_a : Externally applied magnetic field

HTS: High-Temperature Superconductors

I_c : Critical current (the maximum current that a given tape can carry at a given temperature and magnetic field before it reverts to the resistive state).

ISD: Inclined Substrate Deposition

J : Current density

J_c : Critical current density (the value of I_c normalized with the cross-sectional area of the superconducting layer within the tape.)

m : Magnetic moment of a sample

M : Magnetization of the sample material

PVD: Physical Vapor Deposition

QA: Quality Assurance

ReBCO: Rare-earth Barium Copper Oxide

T : Temperature

VSM: Vibrating Sample Magnetometer

VTI: Variable Temperature Insert

w : Tape width



Table contents

1. Introduction: state-of-the art HTS tape material	5
2. Experimental characterization HTS tape material.....	7
2.1 Introduction	7
2.2 Critical current vs magnetic field amplitude and -direction.....	7
2.3 Tape magnetization and ramp-rate dependence	10
2.4 Higher-field campaigns	12
3. Outlook.....	13

1. Introduction: state-of-the art HTS tape material

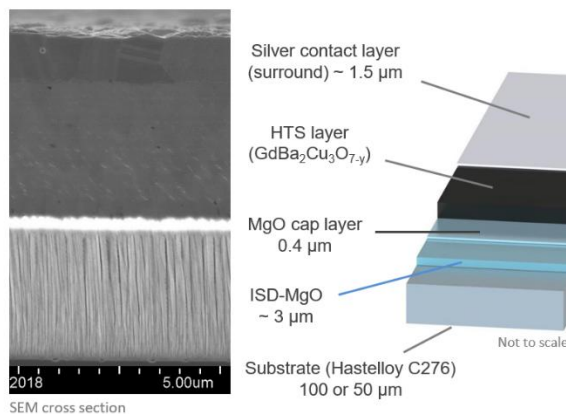
To meet the requirements of the project as efficiently as possible, the HTS tape material should have a critical current density J_c that is maximized for the operational conditions (low temperature T , high magnetic field B , variable magnetic field orientation θ) inside the winding pack of the envisaged magnet coils. Apart from this primary requirement, the material should also have well-controlled and uniform properties in terms of physical dimensions, mechanical strength and thermal behavior.

TH, presently the only EU tape producer, is partner within the project and was identified from the start onwards as the preferred HTS material source. Their basic material architecture consists of a Hastelloy substrate on which MgO buffer layers are ISD-grown. The MgO acts as epitaxial template for a PVD-grown GdBaCuO superconducting layer (Fig. 1). The whole is capped with an Ag layer for chemical protection and with a Cu sheath for thermal/EM stability.

THEVA Pro-Line HTS Wire

THEVA

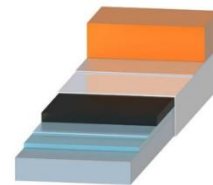
Basic wire architecture



Simple, cost efficient, and robust

Customized wire

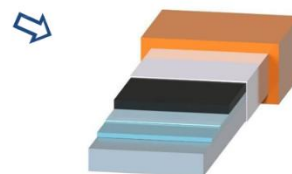
Laminated stabilization



Cu foil laminate
50 -200 μm
Total: 100 - 360 μm

Robust + cost efficient

PVD surround stabilization



Ag, Cu (+PbSn)
up to 10 μm
Total: 65 - 175 μm

High current density

Figure 1. Basic architecture of the TH tape material, with on the **left** the layout of the central basic tape, and on the **right** the different options for implementing the copper stabilization layer.

In order to meet the project requirements that are described above, TH implemented three important changes to their production process:

- *Introduction of artificial pinning centers:* the J_c value of a superconductor is usually determined by its flux-pinning properties, i.e. by the ability of the material to prevent the dissipative redistribution of magnetic flux inside the superconductor. The pinning strength is often determined by naturally occurring crystalline defects that interact with quantized flux lines, but can also be controlled and optimized with artificially grown defects, so-called Artificial Pinning Centers (APC). In ReBCO tapes, these tend to worsen the current performance at higher temperatures, but can significantly enhance J_c at low T and high B (Fig 2).
- *PVD growth of the Cu stabilizer layer:* for optimal control of the tape's cross-sectional size and shape, the external copper layer can be laminated or grown with Physical Vapor Deposition (PVD). Geometrical tolerances become important during coil winding, since they determine the stacking efficiency and the overall current density in the winding pack. TH's base product used to rely on lamination, but the present PVD solution allows for reduced Cu thickness (Fig. 3) and improves control over the overall tape shape and -dimensions.

APC vs Standard HTS

THEVA

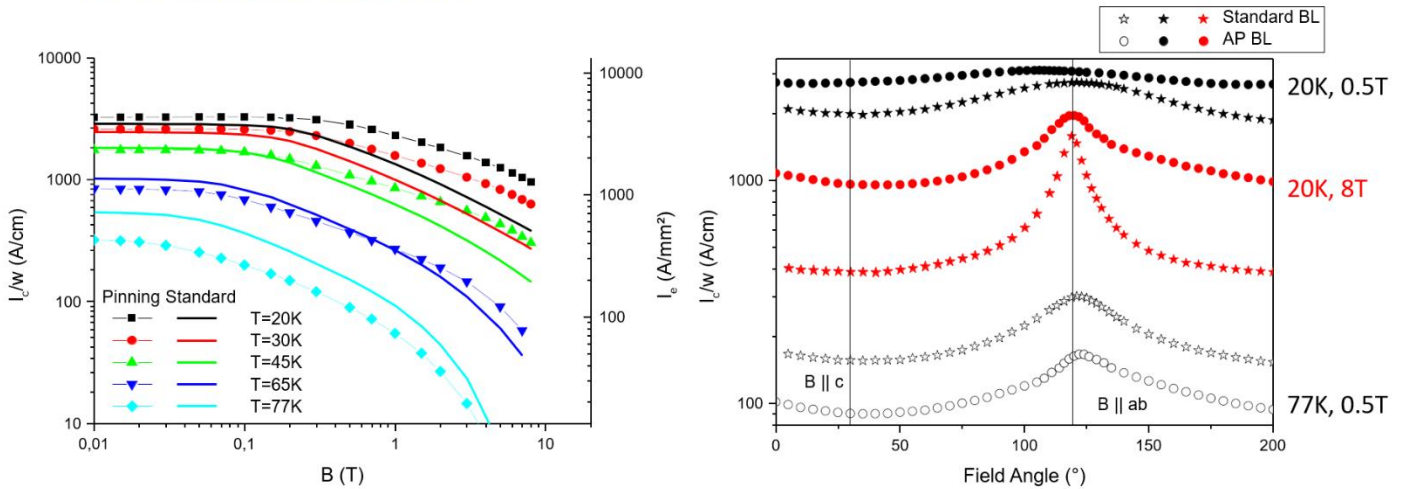
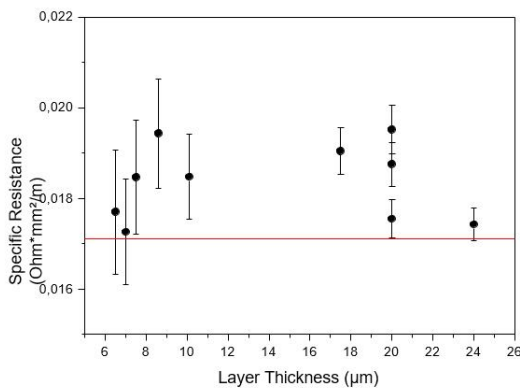


Figure 2. Current-carrying performance as reported by TH for their standard- and APC-material. The graph on the **left** shows J_c (or equivalent I_c/w , the maximum sheet current) as function of B at various T -values. Solid lines represent the standard tapes, symbols the APC ones. The APC significantly enhance the J_c values at lower T and higher B . The graph on the **right** shows I_c/w as function of the orientation of the B -field. In this graph, 0° refers to a magnetic field perpendicular to the flat face of the tapes, stars to the standard material and circles to the APC tapes. The APC reduce the anisotropy at lower T .

- Laser slitting to the required tape width w :** most HTS manufacturers deposit on 12mm-wide substrates, with the resulting tapes able to carry currents of several kA at low T . However, such high current levels are difficult to transfer from a room-temperature power supply into the cryogenic coil environment without creating a significant thermal load. Tape width (and hence operational unit current) is therefore an important design parameter of a stacked-coil type magnet. Narrower tapes allow for more efficient current leads, but necessitate more coils and hence more – possibly cumbersome – coil-to-coil interconnections.

Properties of Cu PVD

THEVA



- Specific resistance of PVD Cu is comparable to Bulk Cu (0.0171 Ohm*mm²/m) showing the high quality of the deposition
- SEM show the surface quality
- SEM cross section show quality of Cu Layer

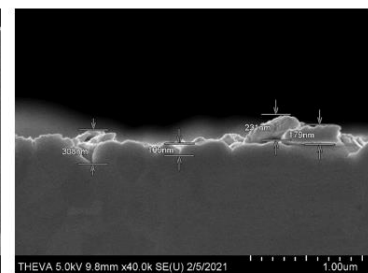
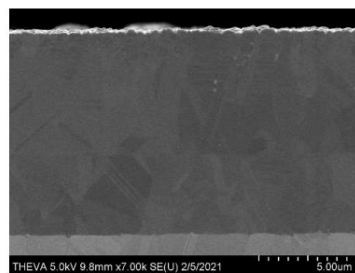
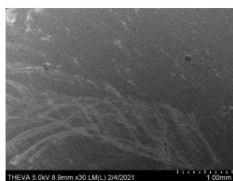


Figure 3. Measured specific electrical resistivity (**top left**) and scanning electron micrographs (**bottom**, both surface and cross-sectional images) of the copper cap layers deposited with the PVD technique. Both the resistivity and the morphology demonstrate the desired high purity and crystallinity required for thermal and electrical transport, as well as the geometry control.

2. Experimental characterization HTS tape material

2.1 Introduction

The main goals of the experimental campaign were two-fold: 1) to obtain an independent confirmation of the current-carrying capacity of the tape material to be used in the magnet coils; and 2) to serve as input for the modelling and design effort in WP4. Focus at UNIGE and UT was on extending the earlier J_c characterization furnished by TH to higher magnetic fields; and at IEE on the inductive determination of the magnetization currents in the tapes. The latter are especially important when modelling the dynamic behaviour of the envisaged HTS coils. Access was also arranged to the high-field facilities at CNRS and at RU in order to extend the data obtained with both resistive and inductive characterisation campaigns to the highly relevant field range $20\text{ T} < B < 30\text{ T}$, where alternative data sources are scarce or – for the APC TH material – completely missing.

2.2 Critical current vs magnetic field amplitude and -direction

Within WP3 (task 3.4) and WP5, it was decided early-on in the project to opt for $w = 6\text{ mm}$ wide tape for the coil winding, basically as a compromise between $w = 12\text{ mm}$ (higher operational current and hence a higher heat load through the main current leads) and $w = 4\text{ mm}$ (lower current but more coils needed for a given stack height, hence more interconnections).

Nonetheless it was agreed that most of the $J_c(B, T, \theta)$ tape characterisation campaign described in this report would be carried out on 4 mm -wide material, since the lower current levels involved are accessible for more experimental set-ups available within the consortium. Therefore, TH distributed 4 mm -wide representative $\text{GdBa}_2\text{Cu}_3\text{O}_7$ APC material with $40\mu\text{m}$ Hastelloy substrate thickness and a $10\mu\text{m}$ thick copper cap layer to the partners involved, together with the corresponding ‘TapeStar’ traces (Fig. 4). These traces are essentially inductively determined recordings of the critical current value at $T = 77\text{ K}$ and are standardly obtained by TH as part of their QA measures during production.

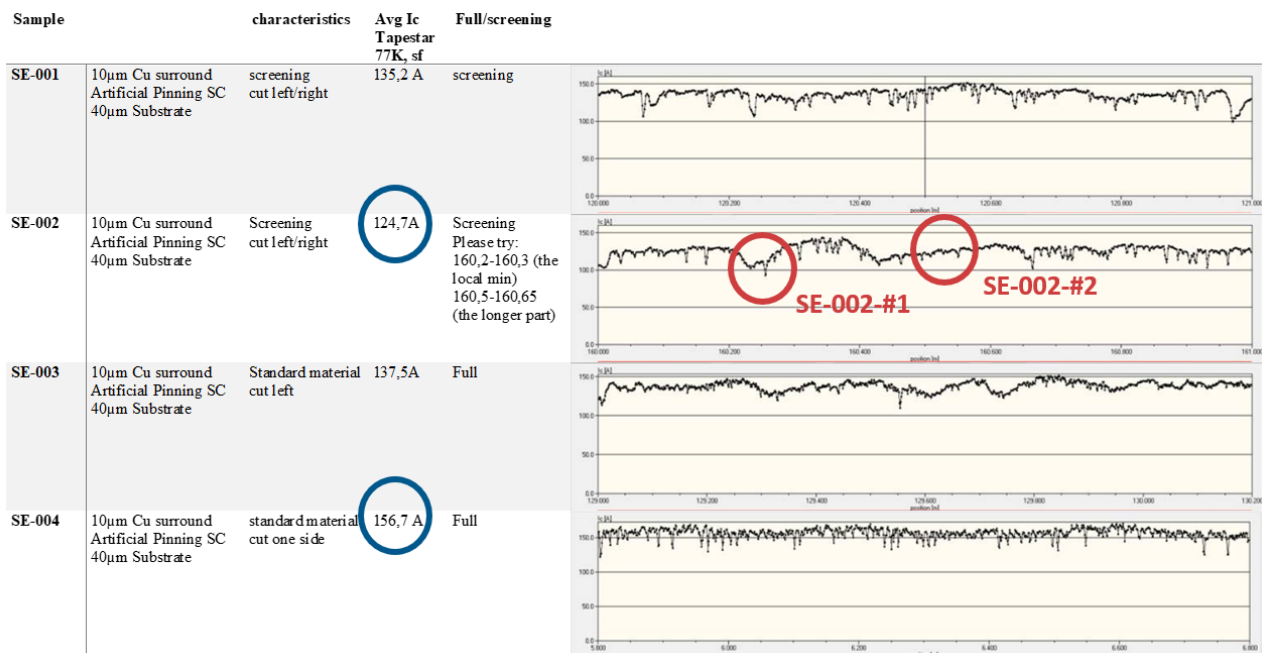


Figure 4. TapeStar traces of some of the 4 mm -wide APC tapes distributed by TH to UNIGE, UT and IEE for further characterization. These traces give the critical current of a tape along its length, inductively measured during production at $T = 77\text{ K}$ in magnetic self-field.

Tape ID	Measurement type	Orientation (wrt tape normal)	Temperature	Field range
SE-001	screening	90°	4.2 K	10 T – 19 T
SE-002-#1 reduced I_c	screening	90°	4.2 K	10 T – 19 T
SE-002-#2 regular I_c	screening	90°	4.2 K	10 T – 19 T
SE-004 High I_c @77 K,sf	expanded	90°	4.2 K 20 K	10 T – 19 T
SE-003/SE-009	full	-15°,0°,15°,90°	4.2 K 20 K	10 T – 19 T

Table 1. Overview of measurements carried out at UNIGE on the 4mm-wide TH material

An extensive set of measurements was carried out at UNIGE (Table 1), who dispose of a 20T solenoidal magnet equipped with a variable temperature insert. With a dedicated sample holder (Fig. 5), current-voltage characteristics up to 1700A can be recorded and the tape sample can be positioned with its wide face under a chosen angle with respect to the applied field direction. The results of these measurements are reported in Figs 6 – 8.

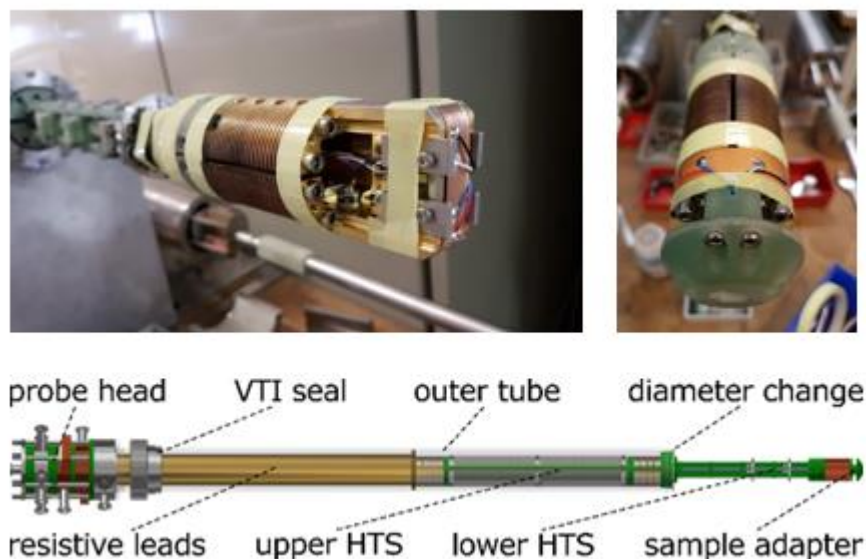


Figure 5. Versatile sample holder for critical current measurements at UNIGE in the bore of a 20 T solenoid equipped with a variable temperature insert (VTI). With the aid of dedicated support pieces, the tape samples can be mounted at selected angles with respect to the solenoidal field.

The data allow to draw several conclusions: 1) the inductive TapeStar results that are routinely recorded by TH in self-field at 77K correlate with the in-field transport data measured at 4.2K; 2) the effectiveness of the APC that was reported by TH for fields up to 8T (Fig. 2) is confirmed to extend also up to fields of 19T; and 3) the anisotropy of the in-field critical current can be adequately described with the aid of a model¹, thus enabling the relatively straightforward prediction of coil performance.

¹ D.K. Hilton et al., *Supercond. Sci Technol.* **28** (2015) 074002.

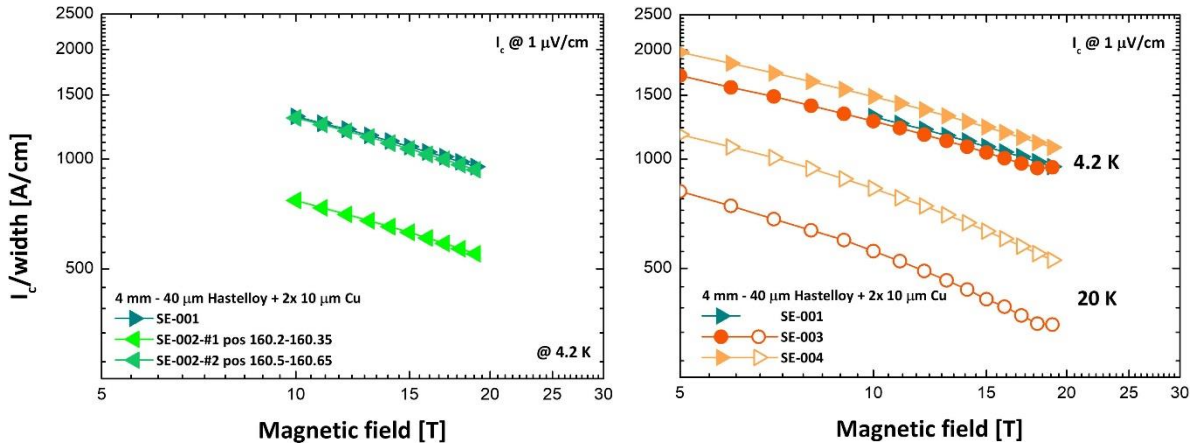


Figure 6. Field dependence of the critical current of TH tapes SE1-SE4, measured by UNIGE in their in-house facility. From tape SE2 two samples were measured (**left graph**), one at a position which the TapeStar trace indicated as anomalous (see Fig. 4). The **right graph** shows the variation of I_c of tapes SE3 and SE4 with temperature.

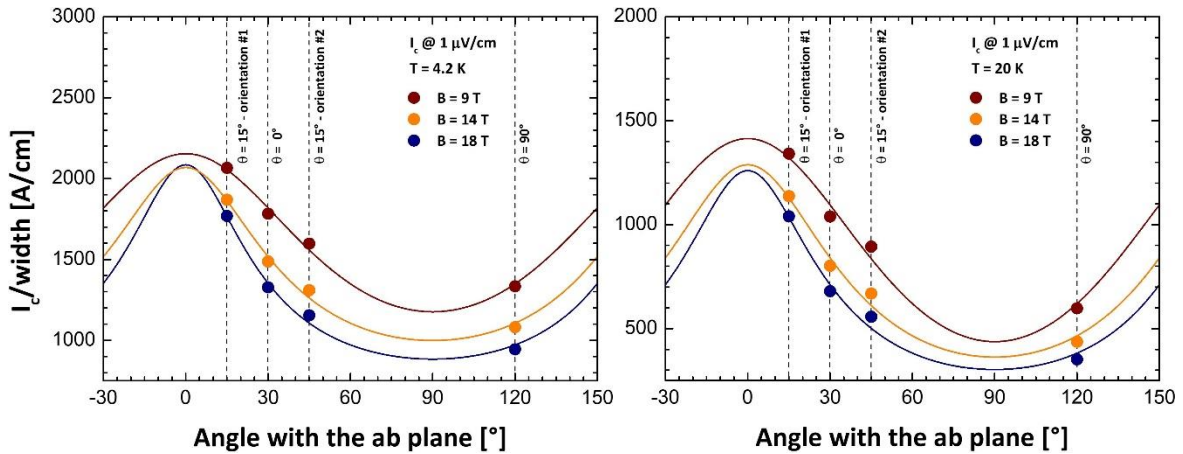


Figure 7. Field-angle dependence of the critical current of TH tape SE3, measured by UNIGE. The data in the **left graph** is recorded at $T=4.2\text{K}$, the data on the **right** at 20K . The θ angle reported at the vertical dashed lines in the plots is the angle between the field and the flat face of the tape, the values on the horizontal axes indicate the angle between the field and the crystallographic ab planes of the epitaxially grown GdBCO layer. The solid lines are model fits.

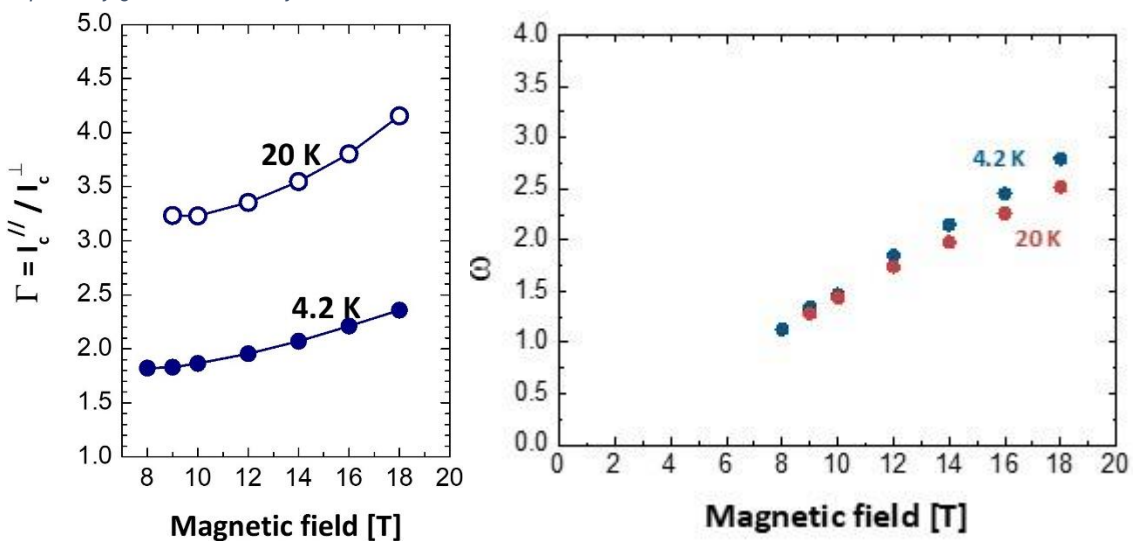


Figure 8. Critical current anisotropy of TH tape SE3 measured by UNIGE. The **left graph** reports the ratio of I_c measured with the magnetic field applied parallel to the flat tape face or perpendicular to it. The **right graph** reports the value of the 'peak sharpness parameter' deduced from the fits in Fig. 7 (see ref. [1] in text).

2.3 Tape magnetization and ramp-rate dependence

Apart from the current-carrying capacity I_c of the tape material, also detailed knowledge of the tape magnetization M in response to an external magnetic field is important for the design of the high-field insert coils. In essence this parameter is indicative of the distribution of the current density J throughout the tape width, which can have an impact on the field homogeneity. Moreover, its ramp-rate dependence reveals the intrinsic relation between J and the value of the electric field E . Inductive magnetization measurements thus allow to investigate lower E levels than those that are experimentally accessible with the more common transport current I – voltage V experiments. Both factors, the internal current distribution and the low-electric-field current density, are directly relevant for the dynamic behaviour of the envisaged coils.

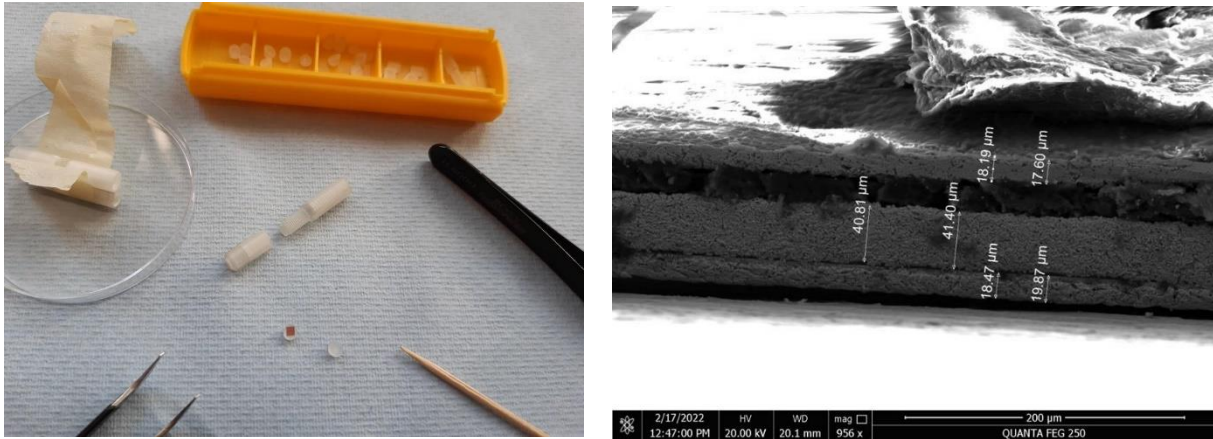


Figure 9. Preparation by IEE of the $(2 \times 2) \text{ mm}^2$ square samples cut from TH tape SE5. The **left** picture shows the sample mounting on a non-magnetic holder, the **right** micrograph illustrates the conservation of the layered tape structure after the cutting.

IEE has extensive experience with the detailed characterization of the magnetization of superconducting materials. M is derived from the precisely measured magnetic moment m of a tape sample in response to an external field. To avoid size-related artefacts, smaller $(2 \times 2) \text{ mm}^2$ samples are cut from the tapes (Fig. 9) and mounted in a vibrating-sample magnetometer (VSM). The VSM stabilizes the sample temperature at a desired value and then sweeps the external field H_a up and

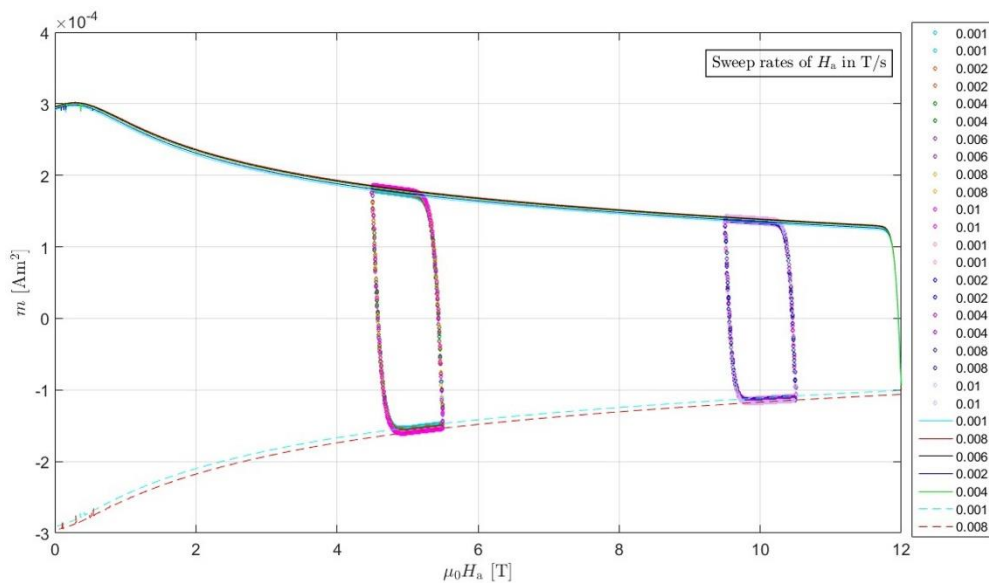


Figure 10. Typical example of an $m(H_a)$ loop recorded at $T = 4.2 \text{ K}$ on a sample cut from TH tape SE5. Apart from the major loop measured during a field excursion to 12T and back, also two minor loops centred at $\mu_0 H_a = 5 \text{ T}$ and 10 T were recorded. These minor loops are taken at various ramp rates (right legend) and allow to reconstruct the electric field dependence of the current density.

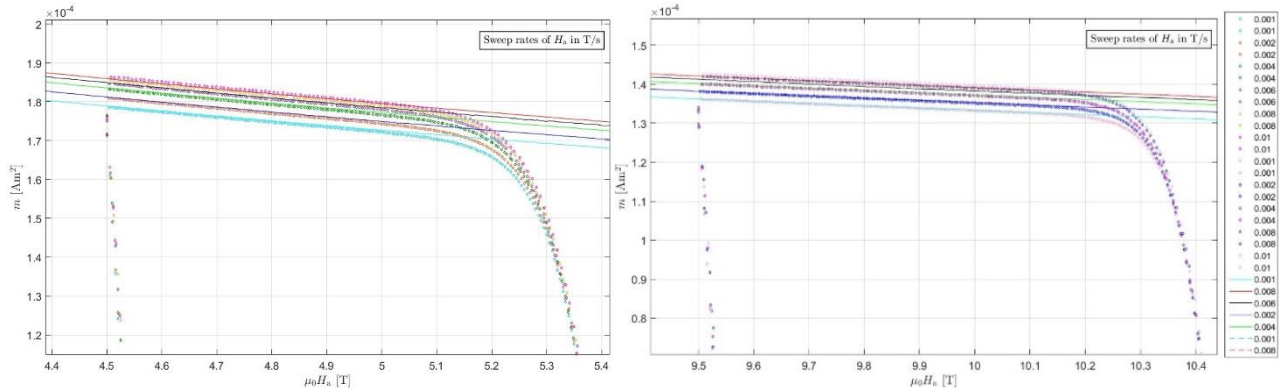


Figure 11. Detailed view of the minor $m(H_a)$ loops obtained at 5T (left) and 10T (right) by IEE on sample SE5 at 4.2K, shown in-full in Figure 10. As expected, the magnitude of the magnetic moment m shows a clear dependence on the field-sweep rate dH_a/dt , which is dictated by the corresponding variation in the induced internal electric field E . m in turn is directly proportional to J .

back down, meanwhile recording the moment m of the oscillating sample with a set of inductive pick-up coils. An example of the resulting $m(H_a)$ loops is shown in Fig. 10.

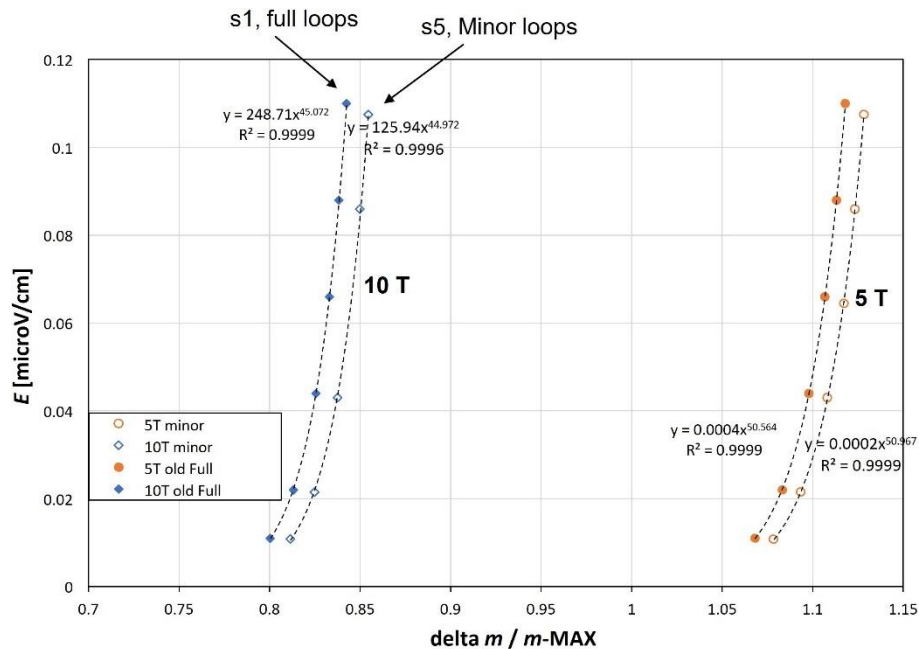


Figure 12. Analysis of the data in Figures 10 & 11 in terms of electric field E (proportional to the external field sweep rate dH_a/dt) vs. the current density (proportional to the 'vertical size' Δm of the minor loops shown in Fig. 10).

The minor loops centred at 5T and at 10T were recorded repeatedly with a range of sweep rates $1\text{mT/s} \leq \mu_0 dH_a/dt \leq 10\text{mT/s}$ (Fig. 11). Through Faraday's law, these sweep rates are directly related to the induced electric field E within the sample, while the magnetization current density J can be derived from the measured magnetic moment m with the aid of the Bean critical state model. These two relations allow to analyse the data in terms of current density – electric field curves (Fig. 12), extending the experimental window that is typically accessible to direct transport current - voltage measurements significantly downwards to lower E -field values.

2.4 Higher-field campaigns

As stated above, the main goal of this tape characterization Task 3.1 is to furnish input to the modelling efforts in WP4, which in turn aim at the design of 32 or 40T class insert coils. Although the data described under §2.2 and §2.3 is undoubtedly useful in this respect, they still must be extrapolated to significantly higher magnetic field levels in order to be able to predict the tape's performance in the envisaged coils.

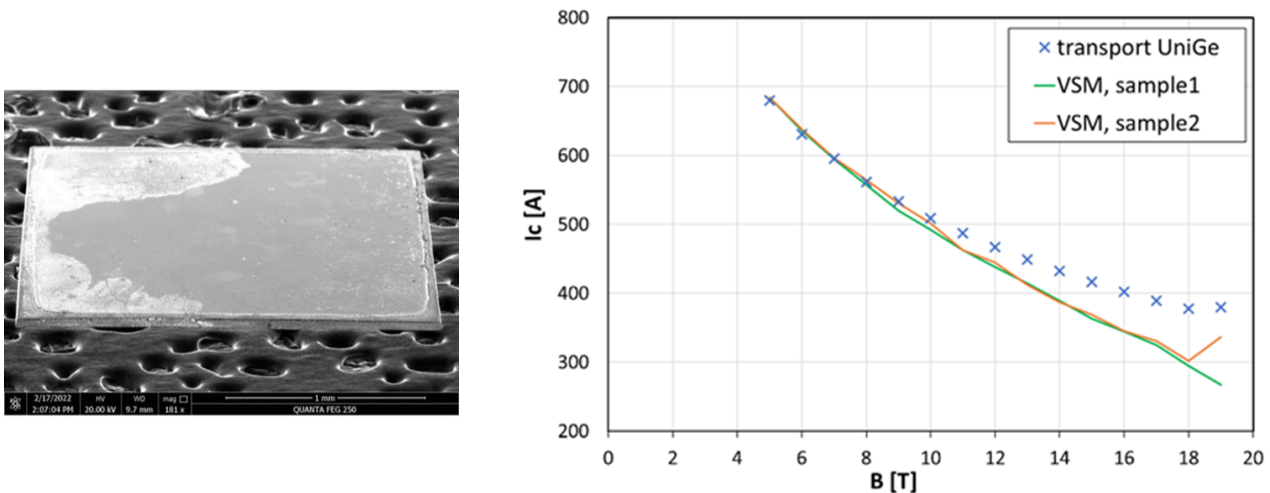


Figure 13. Left: (2×2) mm² sample similar to the ones in Figure 9, but for characterization by IEE in the 30T VSM facility at RU. Right: comparison of the obtained magnetization data at RU (solid lines), analysed in terms of critical current density, with earlier transport data obtained at UNIGE (symbols).

With this in mind, magnet time was requested and awarded in the 30 T Bitter magnet facilities at RU and at CNRS. RU has an existing VSM set-up compatible with their 30 T magnet, which was made available to IEE for a characterisation campaign similar to the one described under §2.3 but at higher

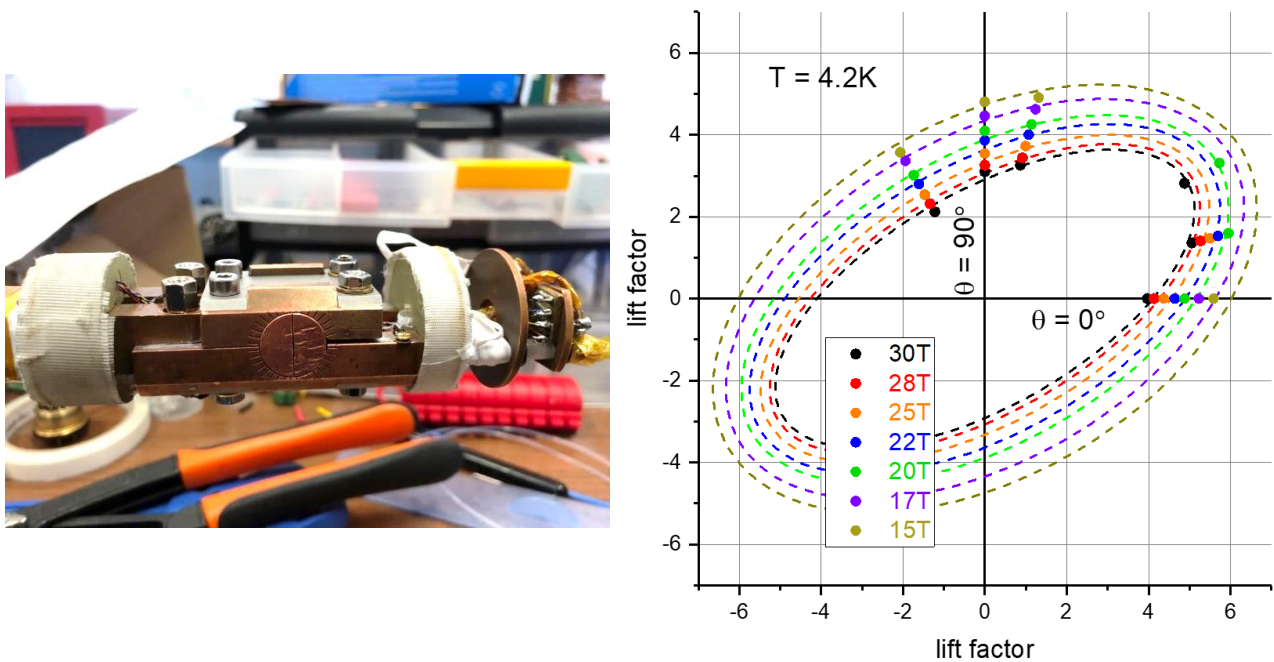


Figure 14. Left: existing sample holder for critical current measurements up to 30T at CNRS. Right: transport measurements by UT and CNRS of TH tape SE8 with this sample holder (symbols). The data are compared to a similar 'elliptic' model (dashed lines) as the one in Figure 7 and are reported as a 'lift factor', i.e. as the ratio between the measured critical current (at 4.2K) at the given field amplitude and -orientation and the I_c -value measured in self-field at 77K. The horizontal and the vertical axes correspond to field directions parallel and perpendicular to the wide tape face, respectively.

magnetic field (Fig. 13). Analogously, at CNRS an existing 30T insert for transport measurements of I_c at variable field angles was made available to UT for extending the data gathered by UNIGE and described under §2.2 to higher fields (Fig. 14). Apart from providing access to their facilities, both RU and CNRS offered extensive assistance during these two measurement campaigns.

Both high-field measurement campaigns encountered unforeseen issues and the resulting data are therefore deemed preliminary. Both issues are being addressed and new measurement campaigns are foreseen (see §3 below).

In the inductive measurements by IEE and RU, at lower magnetic fields good correspondence in I_c value was achieved with the transport data reported by UNIGE, but at fields above $\sim 10T$ both experiments progressively start to deviate from each other (Fig. 13, right). At 18T, the inductive results are about 25% lower than the transport ones. Presumably, this reduction is merely apparent and is due to mechanical noise in the VSM experiment caused by the turbulent flow of the Bitter magnet's cooling water, which tends to induce noise in the magnetic field experienced by the sample and thus lowers its magnetic moment.

In the transport campaign by UT and CNRS similar discrepancies were found with the UNIGE data, albeit for a different reason. In-between measurements at different angles, the sample needs to be warmed up and rotated to a new orientation at room temperature. These cycles resulted in a gradual but progressive degradation of the sample, eventually leading to a $\sim 15\%$ reduction in I_c compared to the UNIGE data. At the writing of this report, the root cause is still under debate (thermal cycling or the sizeable EM shear forces on the sample during the measurements).

3. Outlook

During the first Reporting Period of SuperEMFL, emphasis lay on extending the characterization of the critical current of the selected TH material to low temperatures and high magnetic fields. Although the issues encountered in the higher-field campaigns introduced some uncertainty on the data well above 20T, the effectiveness of the APC in boosting the critical current of the TH tapes at lower temperatures was confirmed also at the highest magnetic fields, while the coil design WP4 was furnished with preliminary input data for the modeling.

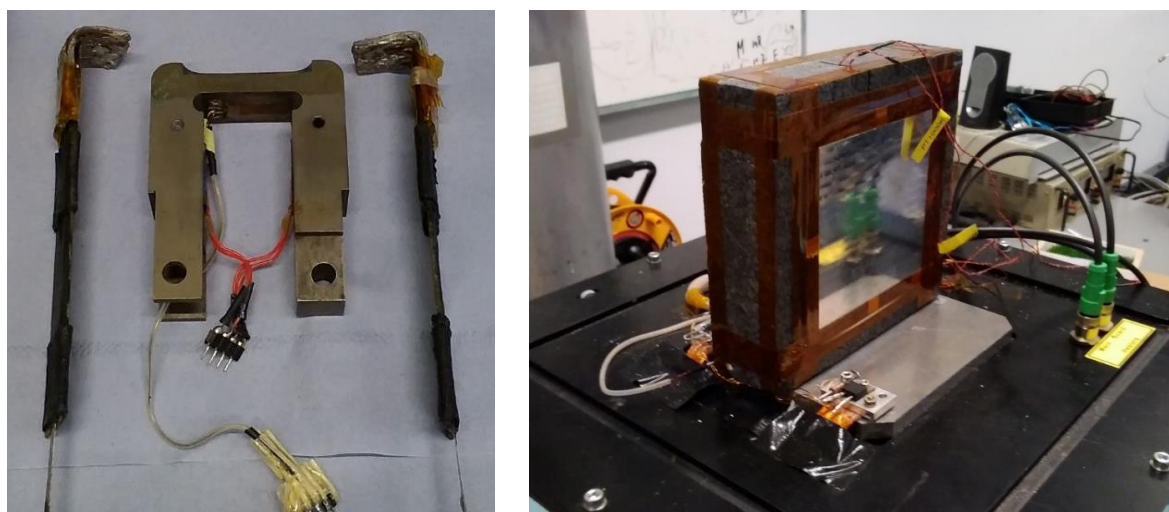


Figure 15. Adaptation of existing set-ups for critical current measurements under axial mechanical strain (left) and transverse thermal conductivity in tape stacks (right) at UT to accommodate the TH sample material.



Characterization in terms of mechanical and thermal properties is under preparation (Fig. 15) and the present report will be updated as these data become available. Similarly, the experience gathered during the higher-field campaigns at RU and CNRS (§2.4) has been used to adopt improved experimental sample holder designs. Assembly of these adapted probes is underway and access to the facilities for follow-up campaigns has been requested/rewarded. Also these new data will be made available as an update to this report. Finally, other tapes from other producers than THEVA will be tested and the publishable results integrated in this report.